JOURNAL OF CHEMICAL & ENGINEERING DATA

ARTICLE

pubs.acs.org/jced

Vapor Pressures and Sublimation Enthalpies of Nickelocene and Cobaltocene Measured by Thermogravimetry

María Teresa Vieyra-Eusebio and Aarón Rojas*

Departamento de Química del Centro de Investigación y de Estudios Avanzados del IPN, Av. Instituto Politécnico Nacional 2508, C.P. 07360, México D.F., Mexico

Supporting Information

ABSTRACT: Vapor pressure data and sublimation enthalpies of organometallic compounds that were measured by thermogravimetry and the application of Langmuir's equation are reported. Herein is a detailed experimental procedure that is applied to nickelocene and cobaltocene. The accuracy and uncertainty for the experimental nickelocene sublimation enthalpy show that the measurement reliability is comparable to the direct calorimetric data that have already been reported for this organometallic compound. Furthermore, the melting temperature and enthalpy as well as the crystal-phase heat capacities between (295 to 420) K for cobaltocene and nickelocene were calorimetrically measured by differential scanning calorimetry (DSC), whereas the gas-phase heat capacities for these metallocenes were theoretically estimated using density functional theory (DFT) calculations.

INTRODUCTION

Experimental quantitation of an organometallic compound's thermochemical properties in the gas phase requires the sublimation enthalpy. This quantity is also important because it is directly related to the intermolecular cohesion energy in the crystalline arrangement, which provides insight into the solid phase energetics and structure.

The sublimation enthalpy can be experimentally measured by direct or indirect methods. The direct methods utilize an appropriate calorimetric technique[1−5] to determine the heat that is associated with the phase change. For substances with a high vapor pressure, the sublimation heat can be calorimetrically quantitated without problems at relatively low temperatures. However, for certain organometallic compounds, such as cobaltocene, an inherently low vapor pressure and compound instability prohibit the long exposure to the experimental temperature that is required to convert the entire sample into gas inside a calorimeter. The more time a cobaltocene sample requires to change phase, the more decomposition products accumulate at the sample surface; vapor pressure then diminishes in proportion to the temperature exposure time. This outcome was observed by the authors for the cobaltocene, when its sublimation enthalpy was unsuccessfully measured using differential scanning calorimetry (DSC) and the methodology described in ref 4.

With indirect methods, a quantity associated with the vapor pressure of the solid is measured at several temperatures, and the heat of sublimation can then be derived from the vapor pressure dependence on the temperature using the Clausius−Clapeyron equation. Examples of indirect techniques are Knudsen's effusion[6−8] and Langmuir's method.[9−15] This last technique is applied in this work using a simultaneous thermogravimetric (TGA)/differential scanning calorimetric (DSC) analyzer and has been demonstrated to be effective. Given the short time required to obtain a complete set of measurements,[10−15] this technique avoids a long sample exposure to relatively high temperatures, which significantly reduces decomposition.

Given its high stability and facility for purification compared with other organometallic compounds, direct and indirect studies of the metallic cyclopentadienyl sublimation process have centered on ferrocene. Therefore, this substance has become a calorimetric reference compound,[16] and its vapor pressure data are also available over a large range of temperatures.[17−21] Herein, ferrocene was used to calibrate the thermogravimetric device, while the nickelocene has been used to test the accuracy and reliability of the experimental procedure and device prior to the cobaltocene measurements.

A detailed description of the experimental procedure is provided, and the experimental results for the sublimation enthalpy are compared with the sparse reported data available. Sublimation enthalpy is usually reported at 298.15 K; therefore, the experimental results were corrected for temperature. For this calculation, the heat capacity of the solid was indispensable, which was measured by DSC, whereas the gas phase heat capacity was theoretically estimated. Furthermore, the melting data for nickelocene and cobaltocene, which were also measured by scanning calorimetry, are reported.

EXPERIMENTAL METHODS AND MATERIALS

The metallocenes studied in this work were commercial samples and, when possible, were purified by sublimation. Ferrocene $[Fe(C_5H_5)_2]$ underwent sublimation twice under reduced pressure, approximately 30 Pa, and at a maximum temperature of 323.15 K; once sublimed it was stored in amber-glass flask. Nickelocene $[Ni(C_5H_5)_2]$ was also purified by two sublimation steps, but in small sample sizes, under a reduced pressure of around 30 Pa, and at a maximum

Special Issue: Kenneth N. Marsh Festschrift

Received: August 6, 2011
Accepted: October 30, 2011
Published: November 10, 2011

Table 1. Chemical Characteristics, Source, and Purity Data of the Substances Utilized

chemical name	molar mass/g·mol^{-1}	source	initial mole fraction purity	purification method	final mole fraction purity	analysis method
ferrocene	186.032	Fluka	≥0.98	sublimation	0.9987 ± 0.0002	DSC
nickelocene	188.879	Aldrich	≥0.98	sublimation	0.9984 ± 0.0008	DSC
cobaltocene	189.119	Strem	≥0.98	none	0.9965 ± 0.0007	DSC
nitrogen	28.013	Infra	0.99997	none		

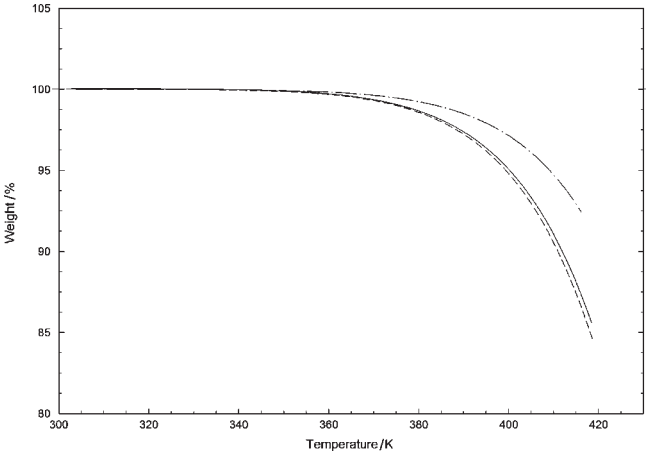

Figure 1. Thermogravimetric curves for the percentage of mass lost as function of temperature. —, Ferrocene calibration; - - -, nickelocene measurement; and — · —, cobaltocene measurement. To obtain these profiles, the heating rate was 10.0 K·min^{-1} for the three compounds, while the nitrogen flow through the furnace was 10.0 cm^3·min^{-1} for ferrocene and nickelocene and 65.0 cm^3·min^{-1} for cobaltocene.

temperature of 328.15 K. The purified compound was then used immediately in the TGA experiments to avoid decomposition during storage. The cobaltocene [$Co(C_5H_5)_2$] was a commercial sample from Strem with a reported mass-fraction purity ≥ 0.98 that was used directly from the supplier's packaging to avoid decomposition from the long heating process that is required for purification by sublimation.

The purity of each metallocene was verified by DSC using a Perkin-Elmer DSC7. All of the melting experiments were performed under a nitrogen atmosphere. For each substance, in a first melting experiment, the calorimeter was programmed to scan over a temperature range from room temperature to 10 K above the melting temperature at a scanning rate of 10.0 K·min^{-1}. This scan was performed to detect any thermal effects in addition to the melting process. No signal was observed over the scanned temperature range prior to the melting peak within the detection limit of the calorimeter. For subsequent melting experiments, the temperature interval for scanning was restricted to a maximum of 10.0 K before and 5.0 K after the melting point and was scanned at a rate of 1.0 K·min^{-1} for the ferrocene and cobaltocene, while the temperature scan was 10.0 K·min^{-1} for nickelocene. From the melting curves, the mole-fraction purities were calculated, and the results are shown in Table 1. The complementary melting temperature and enthalpy data for nickelocene and cobaltocene are described in the Results and Discussion section. The purity of the compounds was also verified by liquid chromatography—mass spectrometry in a LC/MSD-TOF Agilent spectrometer. Chromatograms with a single peak and mass spectra showing the matching mass-to-charge ratio for each metallocene are shown in the Supporting Information.

Thermogravimetry combined with the application of Langmuir's equation has many advantages compared with other indirect techniques for quantitating vapor pressure and the sublimation enthalpy. These advantages include a smaller sample and a shorter experimental time required for a complete set of measurements.[11−14] This methodology is based on Langmuir's equation for determining vapor pressure through sublimation, as follows:[9]

$$(dm/dt)(1/A) = p\gamma\sqrt{M/2\pi RT} \quad (1)$$

In eq 1, dm/dt is the rate of mass loss at temperature T for a sample with an exposed sublimation area A; p is the vapor pressure of the substance; M is the molar mass; R is the gas constant, and γ is a constant of vaporization, which should be close to unity either under vacuum conditions[14] or for compounds with a high molecular mass.[15] For application of eq 1 an accurate measurement of the rate of mass loss as a function of temperature is indispensable and typically obtained using a thermogravimetric analyzer.[11−15]

In this work, a simultaneous TGA/DSC TA Instruments SDT Q600 device was utilized. The sensitive element in this instrument is a dual-beam design thermobalance with a 200 mg sample capacity and 0.1 μg sensitivity; the beams operate inside of a furnace within the range of ambient temperature to 1773 K and a temperature control accuracy of at least ± 1.0 K. Heating rates of (0.1 to 100) K·min^{-1} can be applied to the sample, during which the sample mass change and heat flow can be simultaneously measured. The accuracy of the calorimetric measurements is ± 2 %. The purge gas flow through the furnace can be controlled within a range of (1.0 to 400) cm^3·min^{-1} by a mass flow controller that is integrated into the system.

The system was calibrated for mass with a standard mass that is traceable to the National Institute of Standards and Technology (NIST) and certified as (315.1620 ± 0.0048) mg. The temperature scale was calibrated with reference materials by analyzing the melting temperature of a high-purity indium metal, which had a certified melting temperature traceable to NIST of (429.7485 ± 0.00034) K. Further, the system was calibrated for heat flow by measuring the heat capacity of a certified Sapphire sample and determining the fusion heat for indium that has a certified value of $\Delta_{fus}H$ = (28.51 ± 0.19) J·g^{-1}. The calibration samples were run in heat at 10 K·min^{-1} under a nitrogen flow rate of 100 cm^3·min^{-1}.

To estimate vapor pressure data using the thermogravimetric device, Langmuir's eq 1 can be expressed as follows:

$$p = kv \quad (2)$$

where $k = (2\pi R)^{1/2}/\gamma$ and $v = (1/A)(dm/dt)(T/M)^{1/2}$. Note that, even if the constant γ is not at unity under the experimental conditions, it can be included in the vaporization coefficient k. The vaporization coefficient, in turn, was determined by measuring the rate of mass loss over the temperature range of interest using a reference compound with a known vapor pressure over

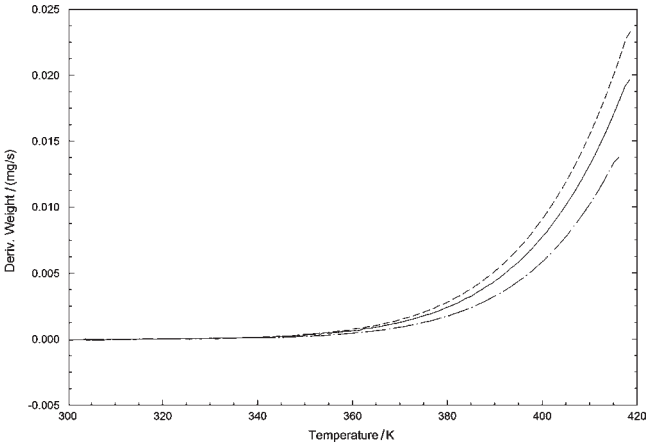

Figure 2. Mass loss derivative curves as function of the temperature, which were used to determine the values for the instantaneous mass loss rate (dm/dt) at temperature T that was required to calculate the vapor pressures in eqs 1 and 2. —, Ferrocene calibration; - - -, nickelocene measurement; and — · —, cobaltocene measurement.

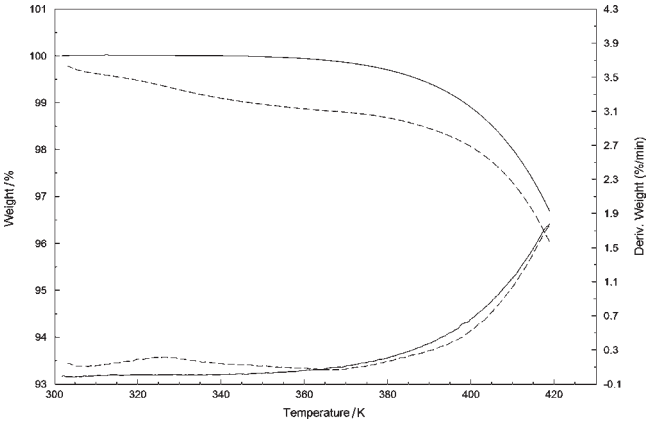

Figure 3. Evolution of the profile for the cobaltocene thermogravimetric curve and its derivative curve through two successive temperature scans. - - -, First scan; —, second scan.

the same temperature range as the nickelocene and cobaltocene measurements. For this purpose, ferrocene can be suggested as an adequate reference compound because it is easily obtainable in a pure state and its vapor pressure has been determined over a wide temperature interval.[17−21] To determine the vaporization coefficient for procedures involving the thermogravimetric device and application of Langmuir's equation, the experiments should be performed with exactly the same procedure and conditions as for nickelocene and cobaltocene, described below.

On base to the sublimation rate of ferrocene utilized as standardizing substance, a mass of approximately 15 mg in the sample cup was established as optimal for the nickelocene experiments. In such tests, the metallocene sample was loaded into TA Instruments in 5.5 mm diameter, 6.0 mm height, and 0.090 cm^3 capacity alumina cups. The thermobalance was tared prior to loading the sample cups. For nickelocene and cobaltocene, the cups were filled with the compound inside a glovebox under a nitrogen gas atmosphere. Once ready, the cup containing the sample was loaded into the sample beam in the SDT Q600 device, and an identical but empty pan was loaded in the

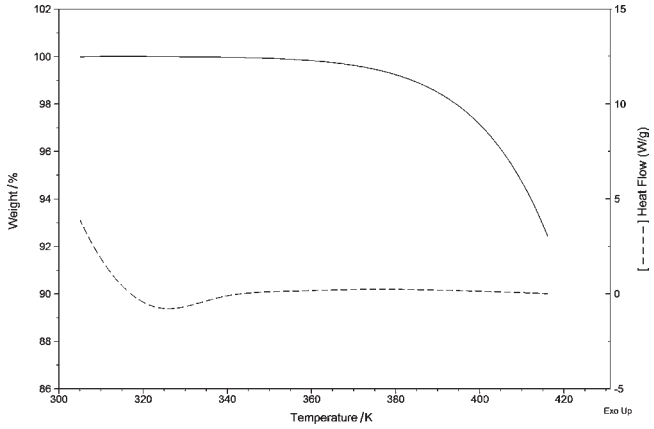

Figure 4. —, Thermogravimetric curve; and - - -, heat flow curve for a representative cobaltocene sublimation experiment.

Table 2. Temperature, Enthalpy, and Purity Data from the Metallocene Melting Experiments Using DSC

m_{sample}	purity	$T_{melting}$	$\Delta^1_{cr}H_m$ ($T_{melting}$)
mg	mole fraction	K	$kJ \cdot mol^{-1}$
		Ferrocene	
7.751	0.9989	448.13	16.1
8.516	0.9987	447.74	16.0
9.074	0.9985	447.93	18.4
7.862	0.9985	447.63	18.5
	0.9987 ± 0.0002	447.9 ± 0.2	17.2 ± 1.4
		Nickelocene	
8.654	0.9991	449.77	18.0
7.024	0.9976	450.05	17.6
4.779	0.9984	450.44	18.4
	0.9984 ± 0.0008	450.09 ± 0.34	18.0 ± 0.4
		Cobaltocene	
4.636	0.9978	450.46	16.8
9.282	0.9962	449.56	17.2
9.058	0.9964	451.29	18.1
10.937	0.9964	450.98	18.6
8.503	0.9958	450.52	18.1
11.158	0.9966	450.31	17.8
	0.9965 ± 0.0007	450.52 ± 0.60	17.8 ± 0.7

reference beam. The TGA/DSC system furnace was closed, and a purge with nitrogen gas at a flow rate of 10 $cm^3 \cdot min^{-1}$ for the nickelocene experiments and 65 $cm^3 \cdot min^{-1}$ for the cobaltocene experiments was activated. These purge gas flow rates were established by many preliminary tests, which sought the best compromise between a low purge gas flow rate and a perceptible and accurately quantifiable loss of mass. Using these purged flow rates, a constant nitrogen gas pressure surrounded the sample to prevent decomposition but without substantially affecting the sample vaporization rate.[15]

Once inside the thermogravimetric system, for thermal stabilization prior to the temperature scan, an equilibration step was programmed at 303 K using the *Thermal Advantage* software of

Table 3. Representative Data Series for the Ferrocene Thermogravimetric Experiments Used To Determine the Vaporization Coefficient k, Associated with Langmuir's Methodology That Was Developed Using the SDT Q600[a]

T	m	$(dm/dt)\cdot 10^9$	$v\cdot 10^3$	P[17,18]
K	mg	$kg\cdot s^{-1}$	$(kg\cdot K\cdot mol)^{1/2}\cdot s^{-1}\cdot m^{-2}$	Pa
Heating Rate, 10.0 $K\cdot min^{-1}$ and Nitrogen Gas Flow Rate, 10.0 $cm^3\cdot min^{-1}$				
348.2	18.7442	0.261	0.48	66
353.2	18.7342	0.389	0.71	94
358.2	18.7201	0.580	1.07	132
363.2	18.6908	0.819	1.52	184
368.2	18.6605	1.170	2.19	254
373.2	18.6172	1.641	3.09	349
378.2	18.5588	2.233	4.24	472
383.2	18.4786	3.053	5.83	636
388.2	18.3703	4.101	7.89	852
393.2	18.2273	5.455	10.56	1127
398.2	18.0347	7.219	14.06	1486
403.2	17.7808	9.489	18.59	1944
408.2	17.4492	12.321	24.29	2523
413.2	17.0125	15.919	31.58	3264
Linear Regression Results Involving 54 Pairs of Data P vs v (see Supporting Information):				
$P/Pa = 104\,814.4v + 32.6$	$r^2 = 0.9995$	$k = 104\,814.4\ (kg\cdot K\cdot mol)^{1/2}\cdot m\cdot s^{-1}$		$u(k) = 0.0002\cdot k$
Heating Rate, 10.0 $K\cdot min^{-1}$ and Nitrogen Gas Flow Rate, 65.0 $cm^3\cdot min^{-1}$.				
353.2	28.3354	0.470	0.86	94
358.2	28.3176	0.685	1.26	133
363.2	28.2933	0.985	1.83	185
368.2	28.2585	1.367	2.56	255
373.2	28.2103	1.910	3.60	348
378.2	28.1411	2.625	4.98	473
383.2	28.0465	3.598	6.87	637
388.2	27.9185	4.863	9.35	852
393.2	27.7498	6.453	12.49	1127
398.2	27.5224	8.553	16.66	1487
403.2	27.2285	11.139	21.83	1940
408.2	26.8393	14.459	28.51	2523
413.2	26.3370	18.568	36.83	3254
Linear Regression Results Involving 53 Pairs of Data P vs v (see Supporting Information):				
$P/Pa = 87\,038.6v + 27.4$	$r^2 = 0.9999$	$k = 87\,038.6\ (kg\cdot K\cdot mol)^{1/2}\cdot m\cdot s^{-1}$		$u(k) = 0.0001\cdot k$

[a] A complete data set for all series is provided in the Supporting Information. The uncertainty is $u(k) = 0.0002\cdot k$, computed as the standard deviation of the slope, σ_b, in the linear regression of all pair of data P vs v.

the Q600 system; this step typically required five to eight minutes. Once thermal equilibrium was reached, the sample was automatically heated at scanning rate of 10 $K\cdot min^{-1}$. This temperature scanning rate was established as optimal through preliminary experiments. Representative curves for the mass loss as function of temperature from the ferrocene calibration and the nickelocene and cobaltocene measurements are shown in Figure 1. The heating rate used promoted a mass loss of approximately 15 % for ferrocene and nickelocene and approximately 8 % for cobaltocene over the temperature interval (303 to 418) K in approximately 12 min. This short time avoids a long exposure to relatively high temperatures and prevents sample decomposition. The thermogravimetric curves are smooth and well-defined, and the corresponding mass losses are sufficient to accurately quantitate the vaporization coefficient k from the ferrocene experiments and to determine the vapor pressures and the sublimation enthalpies for nickelocene and cobaltocene. Note that the curve profiles for ferrocene and nickelocene are similar; both compounds have a perceptible mass loss from sublimation beginning at 345 K. In contrast, the lower vapor pressure of cobaltocene results in an appreciable mass loss beginning near 355 K.

For each experiment, the instantaneous rate of loss of mass dm/dt at temperature T, to substitute in eq 1, was computed from the derivative curve for the loss of mass over time as a function of the temperature. Figure 2 shows these curves, which were generated using the software *Universal Analysis* for the Q600 device from representative experiments with ferrocene, nickelocene, and cobaltocene. Each of the three metallocenes has

a similar profile for the rate of mass lost as the heating of each of the respective sample advances. However, these curves confirm that the quantifiable mass loss for ferrocene and nickelocene began at a lower temperature than for cobaltocene.

It is interesting to note that, for cobaltocene and sometimes for nickelocene, an initial temperature scan between (303 and 418) K was required prior to measuring the mass lost to derive vapor pressures. For that first experiment, the loss of mass curve as a function of temperature and its derivative over time was irregular, as shown in Figure 3. Such irregularity possibly was caused by the quick removal of very small particles and volatile impurities of sample through heating and nitrogen flow of the TGA device, until reaching a homogeneous particle size and a flat exposed surface on the top of the sample. After cooling, to derive the vapor pressures and sublimation enthalpies, the mass loss was measured during a second heating of the same sample, which produced a thermogravimetric curve with the smooth and well-defined profile shown also in Figure 3.

A simultaneous measurement of the calorimetric signal from the SDT Q600, as shown in Figure 4, is useful to verify that the sample is not decomposing during sublimation, particularly for cobaltocene. For experiments with this metallocene, the heat flow curve shows a large negative curvature in the interval (303 to 340) K; this curvature is from the initial heating and the heat capacity difference between the sample-filled cup and empty reference cup in the respective beams. In the temperature interval (340 to 420) K, where according to the thermogravimetric curve the sublimation occurs, no exothermic signals were associated with sample decomposition. A slight negative slope of the heat flow curve in this temperature range is associated with the endothermic sublimation process. This endothermic effect is more evident in an amplified section of the curve shown in the Supporting Information. Also shown in the Supporting Information, the derivative curve for temperature as a function of time for this representative cobaltocene experiment shows that, after the initial heating at the beginning of the experiment, the heating rate is constant after 340 K, and the temperature data are more trustworthy after this point, which justifies the restricted (345 to 413) K range for data analysis.

To confirm that the cobaltocene sample did not decompose after two measurements through 413 K, the purity was verified using DSC for three different samples that were recovered from the alumina cups of the Q600 device after the experiment. The resulting mole fraction was 0.9954, which indicates that purity did not significantly decrease after either the first or second heating through 413 K under the TGA measurement conditions, because of the high rate of heating and consequently the short lapse where the sample is exposed at the high temperature required for its sublimation.

To derive an accurate value for the sublimation enthalpy at 298.15 K from the results at the experimental temperature, reliable data for the gas-phase molar heat capacity of the metallocenes are required, but these values are not available in the literature for the range of temperature involved in this work. Therefore, the heat capacities for solid nickelocene and cobaltocene were measured by DSC using a DSC7 Perkin-Elmer calorimeter that was previously calibrated for energy and temperature with high-purity indium and zinc samples. The heat capacity of each solid metallocene was measured over the range (293.2 to 353.2) K at a 5.0 $K \cdot min^{-1}$ scan rate. These experiments were performed using approximately 20 mg of sample and under a nitrogen flow rate of 30 $cm^3 \cdot min^{-1}$. Prior to the

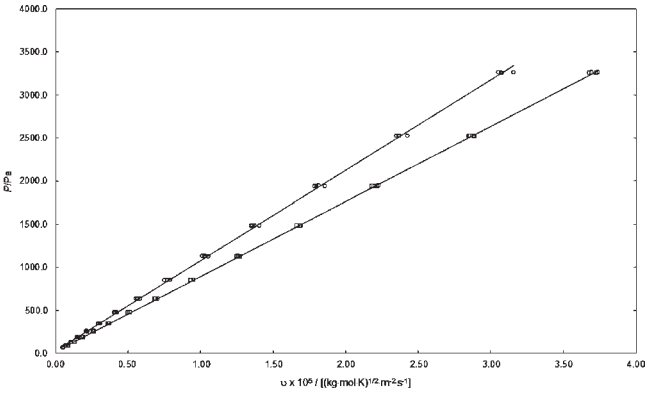

Figure 5. Linear regression of ferrocene vapor pressure data as function of the factor υ to determine the vaporization coefficients k. ○, Experiments under a 10.0 $cm^3 \cdot min^{-1}$ nitrogen flow; $P/Pa = 104\,814.4\upsilon + 32.6$; $r^2 = 0.9995$. □, Experiments under a 65.0 $cm^3 \cdot min^{-1}$ nitrogen flow; $P/Pa = 87\,038.6\upsilon + 27.4$; $r^2 = 0.9999$.

metallocene heat-capacity measurements, the Perkin-Elmer DSC7 calorimeter was tested by measuring the C_p for a high-purity sapphire sample. For this substance, the measured heat capacity was 0.775 $J \cdot K^{-1} \cdot g^{-1}$ at 298.15 K, 0.871 $J \cdot K^{-1} \cdot g^{-1}$ at 350 K, and 0.942 $J \cdot K^{-1} \cdot g^{-1}$ at 400 K compared with the literature values[16] of 0.775 $J \cdot K^{-1} \cdot g^{-1}$ at 298.15 K, 0.872 $J \cdot K^{-1} \cdot g^{-1}$ at 350 K, and 0.943 $J \cdot K^{-1} \cdot g^{-1}$ at 400 K, which means an agreement better than 99.85 %.

Gas-phase heat capacity data were estimated with the deMon[22] program using a density functional formalism[23] and the generalized gradient approximation (GGA) through the exchange-correlation functional of Perdaw and Wang (PW91).[24] The double-Z valence polarization all-electron basis set (DZVP),[25] optimized for the generalized gradient approximation, in combination with auxiliary functions A2, was utilized for the optimization of all structures and the vibrational frequencies analysis. The heat capacities of each metallocene, in the interval of temperature of interest, were computed from the resulting frequencies utilizing the subroutine THERMO of the deMon software, which operates through a procedure detailed elsewhere.[26]

RESULTS AND DISCUSSION

Experimental data and detailed results from the melting experiments for metallocenes, including ferrocene utilized as calibrating substance, are shown in Table 2. The mole-fraction impurity was determined from the melting-temperature depression and applying the method of van't Hoff. The melting temperature was characterized as the peak's onset temperature, whereas the melting enthalpy was determined by integrating the melting curves with a straight baseline. The uncertainty for the average of each melting parameter is the standard deviation. For nickelocene, a strong exothermic effect was immediately observed after the fusion peak; therefore, the accuracy of the resulting melting quantities can be affected because sample decomposition is likely during each melting experiment. For cobaltocene, the accuracy of the results also can be affected because it was difficult to control a small leakage from the sample pans during the melting experiments, even though such pans are designed to the study of high vapor pressure substances. Therefore, the mass of the cell before and after the melting experiment

Table 4. Representative Experimental Data, Vapor Pressure, and Sublimation Enthalpy for Nickelocene in the Temperature Range of (348.2 to 413.2) K, Determined by Thermogravimetry Using Langmuir's Equation.[a] Uncertainties Are $u(\ln P) = \sigma$; $u(P)/\mathrm{Pa} = u(\ln P)\cdot P$; $u(\Delta^{g}_{cr}H_m)/\mathrm{kJ\cdot mol^{-1}} = \sigma_b\cdot(R/10^3)$[b]

T	m	$(dm/dt)\cdot 10^9$	$v\cdot 10^3$	P	$(1/T)\cdot 10^3$	
K	mg	$\mathrm{kg\cdot s^{-1}}$	$\mathrm{(kg\cdot K\cdot mol)^{1/2}\cdot s^{-1}\cdot m^{-2}}$	Pa	$\mathrm{K^{-1}}$	$\ln(P/\mathrm{Pa})$
			Series 1			
348.2	12.4289	0.279	0.50	85	2.87	4.45
353.2	12.4186	0.420	0.76	113	2.83	4.73
358.2	12.4034	0.601	1.10	148	2.79	5.00
363.2	12.3814	0.873	1.61	201	2.75	5.31
368.2	12.3500	1.216	2.26	269	2.72	5.60
373.2	12.3045	1.710	3.20	368	2.68	5.91
378.2	12.2429	2.354	4.43	497	2.64	6.21
383.2	12.1582	3.218	6.10	672	2.61	6.51
388.2	12.0437	4.349	8.30	902	2.58	6.81
393.2	11.8918	5.818	11.17	1204	2.54	7.09
398.2	11.6860	7.738	14.95	1600	2.51	7.38
403.2	11.4135	10.193	19.82	2110	2.48	7.65
408.2	11.0491	13.402	26.22	2781	2.45	7.93
413.2	10.5822	17.326	34.11	3608	2.42	8.19

				σ_b	$\Delta^{g}_{cr}H_m$ (380.7 K)
series	equation	r^2	σ	K	$\mathrm{kJ\cdot mol^{-1}}$
Series 1	$\ln P = 28.5 - 8407.0/T$	0.9985	0.05	93	69.9 ± 0.8
Series 2	$\ln P = 28.4 - 8365.0/T$	0.9983	0.05	100	69.5 ± 0.8
Series 3	$\ln P = 28.5 - 8407.8/T$	0.9988	0.04	84	69.9 ± 0.7
Series 4	$\ln P = 28.7 - 8502.9/T$	0.9991	0.03	75	70.7 ± 0.6
Series 5	$\ln P = 28.9 - 8543.7/T$	0.9993	0.03	67	71.0 ± 0.6
Series 6	$\ln P = 28.5 - 8380.9/T$	0.9989	0.04	80	69.7 ± 0.7
Series 7	$\ln P = 28.5 - 8390.0/T$	0.9992	0.04	68	69.8 ± 0.6
Series 8	$\ln P = 28.3 - 8322.2/T$	0.9982	0.05	103	69.2 ± 0.9
Series 9	$\ln P = 28.4 - 8328.1/T$	0.9984	0.05	97	69.7 ± 0.8

Weighted Average Value: $<\Delta^{g}_{cr}H_m[Ni(C_5H_5)_2, 380.7\ K]>/\mathrm{kJ\cdot mol^{-1}} = 70.1 \pm 0.6$

[a] In all of the experiments, the heating rate was 10 $\mathrm{K\cdot min^{-1}}$. The nitrogen flow through the furnace was 10.0 $\mathrm{cm^3\cdot min^{-1}}$. To compute factor v, the area of the sample was $2.376\cdot 10^{-5}$ $\mathrm{m^2}$, which was calculated from the diameter of the sample cup. [b] σ and σ_b are the standard deviations of the function and the slope, calculated from the least-squares fitting of data $\ln P$ vs $(1/T)$; R is the gas constant. Details in calculation of σ and σ_b and a complete data set for all nine series are provided in the Supporting Information.

was quantified, finding that an average of 6.5 % of the sample mass was lost; then each melting enthalpy result was corrected for this loss.

The coefficient of vaporization associated with the TGA/DSC, which was required to derive the vapor pressures, was determined by four series of measurements of the mass loss in 15 mg of ferrocene samples over a (348.15 to 413.15) K interval and under a nitrogen flow rate of 10.0 $\mathrm{cm^3\cdot min^{-1}}$. A representative series of experimental data, including the calculated factor v, the corresponding ferrocene vapor-pressure data from refs 17 and 18, and the resulting vaporization coefficient k, is shown in Table 3. A combined linear regression for four of these series of measurements and the resulting linear equation and regression factor are shown in Figure 5. To determine the vaporization coefficient for the cobaltocene measurements, three series of measurements were performed using also ferrocene as a reference, but with masses of approximately 30 mg, over the interval (353.2 to 413.2) K under a nitrogen flow rate of 65.0 $\mathrm{cm^3\cdot min^{-1}}$. A representative data set for these measurements is also provided in Table 3, and the resulting linear graph is in Figure 5. Complete data for all series of these experiments are given in the Supporting Information.

As indicated in the Experimental Methods and Materials section, the instantaneous loss of mass at temperature T was determined from the derivative curve for mass loss as a function of time, which was computed from the thermogravimetric measurements using the software *TA Instruments Universal Analysis*. The sample area A, which was required for computation of the factor v, was considered equivalent at the transversal section of the cylindrical alumina cup and then calculated from its internal diameter.

Under a nitrogen flow rate of 10.0 $\mathrm{cm^3\cdot min^{-1}}$, the straight line equation obtained was $P/\mathrm{Pa} = 104\,814.388v + 32.609$, which represents the vaporization coefficient k. The quantity 32.609 Pa is a deviation from eq 2 that is inherent to the experimental procedure and temperature range, but it must be considered to keep the final vapor pressure data as accurate as possible for the

dx.doi.org/10.1021/je200815v |J. Chem. Eng. Data 2011, 56, 5008–5018

Table 5. Representative Experimental Data, Vapor Pressure and Sublimation Enthalpy for Cobaltocene in the Temperature Range of (353.2 to 413.2) K, Determined by Thermogravimetry Using Langmuir's Equation.[a] Uncertainties Are $u(\ln P) = \sigma$; $u(P)/\mathrm{Pa} = u(\ln P)\cdot P$; $u(\Delta^{g}_{cr}H_m)/\mathrm{kJ\cdot mol^{-1}} = \sigma_b\cdot(R/10^3)$[b]

T	m	$(dm/dt)\cdot 10^9$	$v\cdot 10^3$	P	$(1/T)\cdot 10^3$	
K	mg	$\mathrm{kg\cdot s^{-1}}$	$\mathrm{(kg\cdot K\cdot mol)^{1/2}\cdot s^{-1}\cdot m^{-2}}$	Pa	$\mathrm{K^{-1}}$	$\ln(P/\mathrm{Pa})$
			Series 1			
353.2	19.7716	0.271	0.49	70	2.83	4.25
358.2	19.7619	0.397	0.73	91	2.79	4.51
363.2	19.7477	0.573	1.06	119	2.75	4.78
368.2	19.7275	0.806	1.50	158	2.72	5.06
373.2	19.6983	1.121	2.10	210	2.68	5.35
378.2	19.6578	1.572	2.96	285	2.64	5.65
383.2	19.6026	2.143	4.06	381	2.61	5.94
388.2	19.5273	2.910	5.55	510	2.58	6.24
393.2	19.4230	3.952	7.59	688	2.54	6.53
398.2	19.2852	5.277	10.19	914	2.51	6.82
403.2	19.1012	7.029	13.66	1216	2.48	7.10
408.2	18.8537	9.277	18.14	1606	2.45	7.38
413.2	18.5291	12.109	23.82	2101	2.42	7.65

series	equation	r^2	σ	σ_b/K	$\Delta^{g}_{cr}H_m$(383.2 K) / $\mathrm{kJ\cdot mol^{-1}}$
Series 1	$\ln P = 27.9 - 8382.2/T$	0.9977	0.06	122	69.7 ± 1.0
Series 2	$\ln P = 27.7 - 8339.0/T$	0.9976	0.06	123	69.3 ± 1.0
Series 3	$\ln P = 27.7 - 8295.9/T$	0.9988	0.04	86	69.0 ± 0.7
Series 4	$\ln P = 27.5 - 8251.9/T$	0.9983	0.05	104	68.6 ± 0.9
Series 5	$\ln P = 28.0 - 8401.1/T$	0.9984	0.05	101	69.8 ± 0.8
Series 6	$\ln P = 27.7 - 8289.9/T$	0.9989	0.04	82	68.9 ± 0.7
Series 7	$\ln P = 28.0 - 8389.1/T$	0.9986	0.04	96	69.7 ± 0.8

Weighted Average Value: $<\Delta^{g}_{cr}H_m[Co(C_5H_5)_2, 383.2\ K]>/\mathrm{kJ\cdot mol^{-1}} = 69.3 \pm 0.8$

[a] In all of the experiments, the heating rate was 10 $\mathrm{K\cdot min^{-1}}$. The nitrogen flow through the furnace was 65.0 $\mathrm{cm^3\cdot min^{-1}}$. To compute factor v, the area of the sample was $2.376\cdot 10^{-5}$ $\mathrm{m^2}$, which was calculated from the diameter of the sample cup. [b] σ and σ_b are the standard deviations of the function and the slope, calculated from the least-squares fitting of data $\ln P$ vs $(1/T)$; R is the gas constant. Details in calculation of σ and σ_b and complete data set for all seven series are provided in the Supporting Information.

nickelocene. Following the procedure detailed in ref 27, the uncertainty for the slope of this straight line was calculated as ± 312.3 $(\mathrm{J\cdot K^{-1}\cdot mol^{-1}})^{1/2}$, and the y-intercept uncertainty was ± 4.1 Pa. For the experiments under a nitrogen flow rate of 65.0 $\mathrm{cm^3\cdot min^{-1}}$, the resulting vaporization coefficient that was applied to the cobaltocene experiments was $P/\mathrm{Pa} = 87\,038.604v + 27.408$ with a slope uncertainty of ± 139.1 $(\mathrm{J\cdot K^{-1}\cdot mol^{-1}})^{1/2}$ and a y-intercept uncertainty of ± 2.2 Pa.

Vapor pressure data were derived from the described vaporization coefficients and application of eq 2 to the mass loss and temperature data from nine experiments on nickelocene and seven on cobaltocene. Representative data are shown in Tables 4 and 5, while complete experimental and resulting data are provided in the Supporting Information. In the temperature range (343.2 to 418.2) K, within which reliable measurements were performed, the corresponding mass-loss rates were $(10^{-7}$ to $10^{-5})$ $\mathrm{g\cdot s^{-1}}$ for a metallocene sample of approximately 20 mg. These mass-loss rates can be associated with sublimation where the vapor is in an equilibrium condition with its solid.

After the vapor pressure was determined as a function of temperature for each metallocene data set, the sublimation enthalpy was computed from the straight line slope obtained by applying the following integrated Clausius−Clapeyron equation:

$$\ln P = -\Delta^{g}_{cr}H_m/RT + C \quad (3)$$

Detailed results for a representative data set, the slope results, linear regression coefficient, and sublimation enthalpy are in Table 4 for nickelocene and Table 5 for cobaltocene. A complete data set for all series is given in the Supporting Information.

The uncertainty for each sublimation enthalpy value is the standard deviation from fitting, which was calculated as described elsewhere.[27] The average values, $\Delta^{g}_{cr}H_m(T) = (70.1 \pm 0.6)$ $\mathrm{kJ\cdot mol^{-1}}$ for nickelocene and $\Delta^{g}_{cr}H_m(T) = (69.3 \pm 0.8)$ $\mathrm{kJ\cdot mol^{-1}}$ for cobaltocene, were assigned at the midpoint of the experimental temperature interval, which was 380.7 K for the cyclopentadienyl nickel and 383.2 K for the cyclopentadienyl cobalt. These sublimation enthalpy values are the weighted average μ, which was calculated as $\mu = \Sigma(x_i/\sigma_i^2)/\Sigma(1/\sigma_i^2)$, where x_i and σ_i are data of sublimation enthalpy and the standard deviation, respectively. The uncertainty for this weighted average is the

dx.doi.org/10.1021/je200815v | J. Chem. Eng. Data 2011, 56, 5008–5018

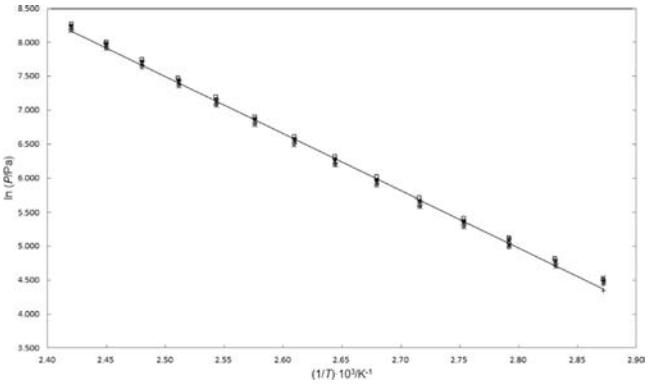

Figure 6. Vapor pressures derived from the thermogravimetric experiments with nickelocene. ◇, Series 1; △, series 2; ○, series 3; ∗, series 4; +, series 5; −, series 6; □, series 7; ×, series 8; ●, series 9. The standard deviations of the fitting associated with the regression over all data are σ = 0.06 and σ_b = 38 K. Uncertainties are $u(\ln P) = \sigma$; $u(P)$/Pa = $u(\ln P)\cdot P$; $u(\Delta^g_{cr}H_m)$/kJ·mol^{-1} = $\sigma_b\cdot(R/10^3)$.

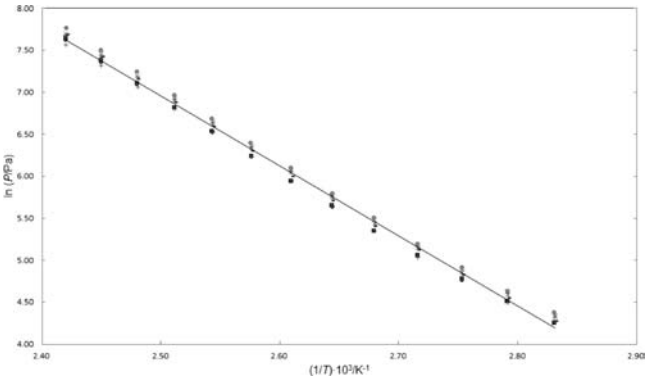

Figure 7. Vapor pressures derived from the thermogravimetric experiments with cobaltocene. ■, Series 1; ●, series 2; ∗, series 3; +, series 4; −, series 5; ×, series 6; ◆, series 7. The standard deviations of the fitting associated with the regression over all data are σ = 0.07 and σ_b = 60 K. Uncertainties are $u(\ln P) = \sigma$, $u(P)$/Pa = $u(\ln P)\cdot P$, $u(\Delta^g_{cr}H_m)$/kJ·mol^{-1} = $\sigma_b\cdot(R/10^3)$.

standard deviation σ, which was computed as $\sigma^2 = N\sigma_\mu^2 = N[1/\Sigma(1/\sigma_i^2)]$, where σ_μ is the standard deviation of the mean for N sublimation enthalpy data.[27]

Linear regression of all of the data sets, shown in Figures 6 and 7, demonstrates the best dependence between vapor pressure and temperature for nickelocene and cobaltocene, respectively. For the nickelocene, the resulting equation is

$$\ln(P/\text{Pa}) = 28.5 - 8402.4(1/T) \quad (4)$$

which is valid for the interval (348.2 to 413.2) K and has a r^2 = 0.9975 regression coefficient. For this equation, the uncertainty in the slope was ± 37.8 K, and the y-intercept uncertainty was ± 0.1. The uncertainty in ln P is 0.06 and represents the standard deviation of the fitting,[27] which implies an uncertainty of 0.06P in the values of vapor pressure. The sublimation enthalpy that was derived from this equation is 69.9 ± 0.3 kJ·mol^{-1}, as expected, which is similar to the calculated average weight of the values derived from the slope of each series, but with a lower uncertainty.

For cobaltocene, the dependence of vapor pressure on temperature is given in the following equation:

$$\ln(P/\text{Pa}) = 27.8 - 8335.6(1/T) \quad (5)$$

which was calculated from linear regression of the seven data sets for this metallocene, is valid for the interval (353.2 to 413.2) K, and has a regression coefficient of r^2 = 0.9954. For this equation, the slope uncertainty was ± 59.8 K, and the y-intercept uncertainty was ± 0.2. Uncertainty in ln P is 0.07 and represents the standard deviation of the fitting,[27] which implies an uncertainty of 0.07P in the values of vapor pressure. The sublimation enthalpy that was derived from this equation is 69.3 ± 0.5 kJ·mol^{-1}, which is identical to the calculated average weight derived from the slope of each series, but with a lower uncertainty. The dispersion was low because once the optimal experimental conditions have been established, the mass loss (dm/dt) data are reproducible for a specific temperature T, both parameters being accurately measured using the TGA/DSC device. This reproducibility is reflected in the almost superimposed ln P versus $1/T$ linear series in Figures 6 and 7.

A comparison of nickelocene vapor pressure data herein with data obtained by Turnbull[28] is shown in Figure 8. As shown, the

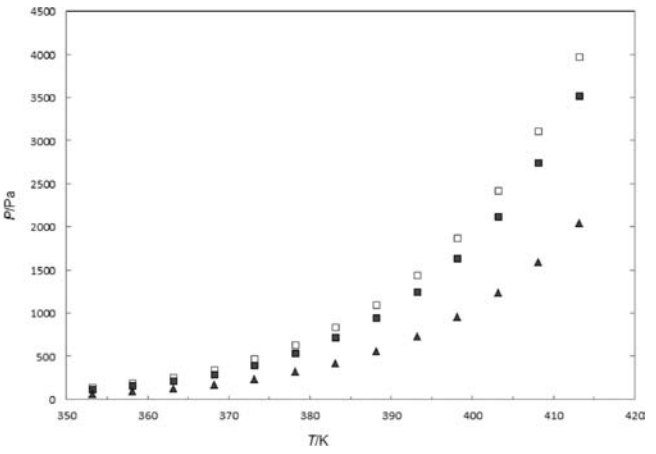

Figure 8. Comparison of the vapor-pressure data P at the temperature T, determined in this work with those data reported in the literature. □, Nickelocene, ref 28; ■, nickelocene, this work; ▲, cobaltocene, this work.

application of Langmuir's equation and the TGA device generated metallocene vapor pressure values that are consistent with previously reported data. For cobaltocene, to the best of our knowledge, no vapor pressure data have been generated in the temperature range of the measurements herein; thus, a comparison is not possible.

To correct the sublimation enthalpy values for temperature, the solid-phase heat capacity was measured for each metallocene using DSC over the temperature range (295 to 415) K, and the values are shown in Table 6. These data were fitted to the equation $C_{p,m}/(\text{J}\cdot\text{K}^{-1}\cdot\text{mol}^{-1}) = a + bT + cT^2$ with a correlation coefficient that was greater than 0.9950. Gas-phase heat capacity data were computed from the DFT frequency analysis and are shown also in Table 6. For compatibility, the gas-phase data were adjusted to a quadratic dependence over the same interval as the solid phase.

From the quadratic equations in Table 6, the computed heat capacity changes for metallocene sublimation processes over the interval 295 to 415 K are $\Delta^g_{cr}C_{p,m}/(\text{J}\cdot\text{K}^{-1}\cdot\text{mol}^{-1}) = -1.44\cdot10^1 - 8.21\cdot10^{-2}(T/\text{K}) + 9.62\cdot10^{-5}(T/\text{K})^2$ for nickelocene and

Table 6. Solid- and Gas-Phase Heat Capacities of Nickelocene and Cobaltocene at Constant Pressure. Uncertainties Are $u[C_p(\text{gas})] = 0.04C_p(\text{gas})$;[a] $u[C_p(\text{solid})] = 0.02C_p(\text{solid})$[b]

	nickelocene		cobaltocene	
T	C_p(solid)	C_p(gas)	C_p(solid)	C_p(gas)
K	$J\cdot K^{-1}\cdot mol^{-1}$	$J\cdot K^{-1}\cdot mol^{-1}$	$J\cdot K^{-1}\cdot mol^{-1}$	$J\cdot K^{-1}\cdot mol^{-1}$
295	198.9	172.2	195.5	171.6
298.15	203.0	173.9	196.9	173.4
300	204.4	175.0	197.1	174.6
305	209.5	177.9	197.6	177.5
310	212.9	180.7	197.8	180.5
315	216.1	183.5	198.4	183.4
320	218.7	186.4	200.3	186.3
325	221.4	189.2	201.6	189.2
330	223.8	192.0	203.9	192.1
335	226.5	194.8	206.5	195.
340	229.5	197.5	209.7	197.8
345	232.1	200.3	212.8	200.6
350	234.6	203.0	216.0	203.4
355	237.2	205.7	220.5	206.2
360	239.9	208.4	225.2	209.0
365	242.3	211.1	230.2	211.7
370	245.0	213.7	232.4	214.4
375	247.0	216.4	235.4	217.0
380	247.0	219.0	239.8	219.7
385	252.0	221.5	245.5	222.3
390	254.6	224.1	250.6	224.9
395	257.2	226.6	256.1	227.4
400	261.0	229.1	262.1	230.0
405	264.0	231.6	268.5	232.5
410	266.9	234.0	274.8	234.9
415	271.0	236.5	282.5	237.4

$C_p/(J\cdot K^{-1}\cdot mol^{-1}) = 1.97\cdot 10^1 + 8.96\cdot 10^{-1}(T/K) - 4.86\cdot 10^{-4}(T/K)^2$

$C_p/(J\cdot K^{-1}\cdot mol^{-1}) = -3.41\cdot 10^1 + 8.14\cdot 10^{-1}(T/K) - 3.90\cdot 10^{-4}(T/K)^2$

$C_p/(J\cdot K^{-1}\cdot mol^{-1}) = 6.34\cdot 10^2 - 3.05\cdot 10^0(T/K) + 5.31\cdot 10^{-3}(T/K)^2$

$C_p/(J\cdot K^{-1}\cdot mol^{-1}) = -4.94\cdot 10^1 + 8.91\cdot 10^{-1}(T/K) - 4.81\cdot 10^{-4}(T/K)^2$

[a] See ref 26. [b] Usual for measurements in the DSC7 scanning calorimeter.

$\Delta^g_{cr}C_{p,m}/(J\cdot K^{-1}\cdot mol^{-1}) = -6.83\cdot 10^2 + 3.94\cdot 10^0(T/K) - 5.79\cdot 10^{-3}(T/K)^2$ for cobaltocene.

From these $\Delta^g_{cr}C_{p,m}$ values, the sublimation enthalpies that were measured at the experimental temperature T were adjusted to the reference temperature 298.15 K using the following equation:

$$\Delta^g_{cr}H_m(298.15\ \text{K}) = \Delta^g_{cr}H_m(T) - \int_{298.15\text{K}}^{T} \Delta^g_{cr}C_{p,m}\, dT \quad (6)$$

Propagation of error analysis, as described elsewhere,[27] showed that the uncertainty associated with the average value of sublimation enthalpy at 298.15 K increases just 0.1 $kJ\cdot mol^{-1}$ with respect to the uncertainty at the experimental temperature T as a result of the usually low dispersion in the DSC temperature and heat-capacity data.

A summary and comparison of the sublimation enthalpy data at the experimental temperature T and 298.15 K, as well as of melting and heat capacity data, are supplied in Table 7. Considering the uncertainty, the $\Delta^g_{cr}H_m$ nickelocene result obtained in this work using thermogravimetry is similar to those previously measured by other indirect techniques[7,10] and is identical to that measured by calorimetry[10] and to that of Turnbull[28] derived from vapor pressure measurements. These measurements may overlap because the experimental conditions were appropriate to promote slow sublimation for this metallocene, which permitted equilibrium between the solid and gas phases with representative vapor pressures of the sample in the entire experimental temperature range. These data suggest that using the described TGA/DSC system and experimental conditions herein, the dependence of increasing vapor pressure with temperature can be followed accurately by the sample mass loss, providing in turn, an accurate result of the sublimation enthalpy.

For cobaltocene, the sublimation enthalpy that was derived from the indirect methodology is only 1.7 $kJ\cdot mol^{-1}$ lower that the value reported by Torres et al.,[7] who determined this quantity for cyclopentadienyl cobalt from Knudsen effusion. However, if a correction of the experimental results to 298.15 K is performed utilizing the correlation $\Delta^g_{cr}H_m(298.15\ \text{K}) = \Delta^g_{cr}H_m(T) + 0.0320(T - 298.15\ \text{K})$, as suggested by Chickos et al.,[29] the results are $\Delta^g_{cr}H_m(298.15\ \text{K}) = 72.7\ kJ\cdot mol^{-1}$ for nickelocene

Table 7. Summary and Comparison of the Results of the Enthalpy of Sublimation, Melting, and Heat Capacity Data for Nickelocene and Cobaltocene

Sublimation Data				
		T	$\Delta^{g}_{cr}H_m(T)$	$\Delta^{g}_{cr}H_m(298.15\ K)$
author	experimental procedure	K	kJ·mol^{-1}	kJ·mol^{-1}
		Nickelocene		
Torres-Gomez et al.[7]	Knudsen effusion	283.4−305.7	71.5 ± 0.6	71.4 ± 0.6
Rojas and Vieyra-Eusebio[10]	Langmuir's method	323.15−333.15	70.4 ± 1.1	71.3 ± 1.1
Rojas and Vieyra-Eusebio[10]	DSC	333.15	71.4 ± 1.3	72.6 ± 1.3
Turnbull[28]	vapor pressure measurements	353.0−419.0		72.4 ± 1.3
this work	thermogravimetry	348.15−413.15	70.1 ± 0.6	72.6 ± 0.7
		Cobaltocene		
Torres-Gomez et al.[7]	Knudsen effusion	296.53−324.54	72.1 ± 0.1	72.3 ± 0.1
this work	thermogravimetry	353.15−413.15	69.3 ± 0.8	70.6 ± 0.9
Melting and Heat Capacity Data				
		$T_{melting}$	$\Delta^{1}_{cr}H_m(T)$	$C_{p,m}(298.15\ K)$
author	procedure	K	kJ·mol^{-1}	kJ·mol^{-1}
		Nickelocene		
Rojas and Vieyra-Eusebio[10]	DSC	450.8 ± 0.4	19.0 ± 0.4	203.2
Rabinovich et al.[30]	adiabatic calorimetry			205.4
this work	DSC	450.1 ± 0.3	18.0 ± 0.4	203.1
		Cobaltocene		
Rabinovich et al.[30]	adiabatic calorimetry			197.3
this work	DSC	450.5 ± 0.6	17.8 ± 0.7	196.9

and $\Delta^{g}_{cr}H_m(298.15\ K) = 72.0$ kJ·mol^{-1} for cobaltocene, which means an excellent agreement with the values proposed by Torres et al.

As shown in Table 7, the nickelocene melting and heat capacity data agree with the few values available in the scientific literature. For cobaltocene, to the best of our knowledge, no previous melting data have been reported. Thus, the only comparison is with Rabinovich et al.'s[30] C_p data, which shows that our data agree well with the heat capacity value at 298.15 K.

Note that, at 298.15 K, a slightly lower sublimation enthalpy was obtained for the cobaltocene than nickelocene. This small difference between the heat of sublimation values of nickelocene and cobaltocene is congruent with the observation that in the solid state both compounds are characterized by a monoclinic structure at room temperature,[31,32] with crystals having a very small difference in the molecular packing forces.[32] Into the crystal both metallocenes present a disordered staggered molecular structure of D_{5d} symmetry, with four and two orientations between the cyclopentadienyl rings, for nickelocene[33] and cobaltocene, respectively.[32]

CONCLUSION

The result of enthalpy of sublimation of metallocenes studied herein show that the indirect technique, by applying Langmuir's equation to mass loss data acquired by the TGA/DSC device while heating the sample, is able to generate representative vapor pressure data and derive good quality results for the sublimation enthalpy for these types of substances. The sublimation heat results are similar in accuracy to those measured by other either indirect or calorimetric techniques, but with a higher reproducibility.

The results herein agree with the values reported in the literature for nickelocene and cobaltocene sublimation enthalpies; the method is easily developed and generates low dispersion, and the measurements can be completed in a short time. These characteristics suggest that this experimental procedure can be applied to accurately determine the sublimation enthalpy of volatile and nonvolatile metallocene compounds when either calorimetric or other indirect procedures are not applicable because the compound is unstable.

ASSOCIATED CONTENT

Supporting Information. Ferrocene vapor pressure data as a function of temperature and complete data series for the ferrocene thermogravimetric experiments used to determine the vaporization coefficient associated with the SDT Q600; also, a complete and detailed experimental thermogravimetric data series for calculated vapor pressure and sublimation enthalpy for nickelocene and cobaltocene. LC-MS chromatographic and spectra data there supplied the corroborate purity of the metallocenes. This material is available free of charge via the Internet at http://pubs.acs.org.

AUTHOR INFORMATION

Corresponding Author

*E-mail: arojas@cinvestav.mx. Tel.: +55 5747 3726. Fax: +55 5747 3389.

Funding Sources

The authors are grateful to CONACYT (Mexico) for financial support (Grants 104299 and 128411) and the scholarship granted to M.T.V.-E.

■ ACKNOWLEDGMENT

Thanks to Geiser Cuellar for LC-MS experiments.

■ REFERENCES

(1) Sabbah, R.; Antipine, I.; Coten, M.; Davy, L. Quelques Reflexions a Propos de la Mesure Calorimetrique de l'Enthalpie de Sublimation ou Vaporisation. *Thermochim. Acta* **1987**, *115*, 153–165.

(2) Santos, L. M. N. B. F.; Schröder, B.; Fernandes, O. O. P.; Ribeiro da Silva, M. A. V. Measurement of Enthalpies of Sublimation by Drop Method in a Calvet type Calorimeter: Design and Test of a New System. *Thermochim. Acta* **2004**, *415*, 15–20.

(3) Torres-Gómez, L. A.; Barreiro-Rodríguez, G.; Galarza-Mondragón, A. A New Method for the Measurement of Enthalpies of Sublimation Using Differential Scanning Calorimetry. *Thermochim. Acta* **1988**, *124*, 229–232.

(4) Rojas-Aguilar, A.; Orozco-Guareño, E.; Martinez-Herrera, M. An Experimental System for Measurement of Enthalpies of Sublimation by D.S.C. *J. Chem. Thermodyn.* **2001**, *33*, 1405–1418.

(5) Rojas-Aguilar, A.; Orozco-Guareño, E. Measurement of the Enthalpies of Vaporization and Sublimation of Solids Aromatic Hydrocarbons by Differential Scanning Calorimetry. *Thermochim. Acta* **2003**, *405*, 93–107.

(6) Torres, L. A.; Gudiño, R.; Sabbah, R.; Guardado, J. A. Standard Reference Material Proposed for Enthalpy of Sublimation Measurements. A Comparative Study of the Standard Molar Enthalpy of Sublimation of $Fe(c\text{-}C_5H_5)_2$(Ferrocene) by Calorimetry and Knudsen-Effusion Techniques. *J. Chem. Thermodyn.* **1995**, *27*, 1261–1266.

(7) Torres-Gomez, L. A.; Barreiro-Rodriguez, G.; Mendez-Ruiz, F. Vapour Pressures and Enthalpies of Sublimation of Ferrocene, Cobaltocene and Nickelocene. *Thermochim. Acta* **1988**, *124*, 179–183.

(8) Santos, L. M. N. B. F.; Lima, L. M. S. S.; Lima, C. F. R. A. C.; Magalhães, F. D.; Torres, M. C.; Schröder, B.; Ribeiro da Silva, M. A. V. New Knudsen Effusion Apparatus with Simultaneous Gravimetric and Quartz Crystal Microbalance Mass Loss Detection. *J. Chem. Thermodyn.* **2011**, *43*, 834–843.

(9) Langmuir, I. The Vapor Pressure of Metallic Tungsten. *Phys. Rev.* **1913**, *2*, 329–342.

(10) Rojas, A.; Vieyra-Eusebio, M. T. Enthalpies of Sublimation of Ferrocene and Nickelocene Measured by Calorimetry and the Method of Langmuir. *J. Chem. Thermodyn.* **2011**, *43*, 1738–1747.

(11) Price, D. M. Vapor Pressure Determination by Thermogravimetry. *Thermochim. Acta* **2001**, *367*, 253–262.

(12) Pena, R.; Ribet, J. P.; Maurel, J. L.; Valat, L.; Lacoulonche, F.; Chauvet, A. Sublimation and Vaporisation Processes of S(−) Efaroxan Hydrochloride. *Thermochim. Acta* **2003**, *408*, 85–96.

(13) Pieterse, N.; Focke, W. W. Diffusion-Controlled Evaporation Through a Stagnant Gas: Estimating Low Vapour Pressures from Thermogravimetric Data. *Thermochim. Acta* **2003**, *406*, 191–198.

(14) Wright, S. F.; Dollimore, D.; Dunn, J. G.; Alexander, K. Determination of the Vapor Pressure Curves of Adipic Acid and Triethanolamine Using Thermogravimetric Analysis. *Thermochim. Acta* **2004**, *421*, 25–30.

(15) Phang, P.; Dollimore, D.; Evans, S. J. A Comparative Method for Developing Vapor Pressure Curves Based on Evaporation Data Obtained from a Simultaneous TG−DTA Unit. *Thermochim. Acta* **2002**, *392*, 119–125.

(16) Xu-wu, A.; Chickos, J. S.; Planas Leitão, M. L.; Roux, M. V.; Torres, L. A.; Sabbah, R. Reference Materials for Calorimetry and Differential Thermal Analysis. *Thermochim. Acta* **1999**, *331*, 93–204.

(17) Kaplan, L.; Kester, W. L.; Katz, J. J. Some Properties of Iron Biscyclopentadienyl. *J. Am. Chem. Soc.* **1952**, *74*, 5531–5532.

(18) Jacobs, M. H. G.; Van Ekeren, P. J.; De Kruif, C. G. The Vapour Pressure and Enthalpy of Sublimation of Ferrocene. *J. Chem. Thermodyn.* **1983**, *15*, 619–623.

(19) Emel'yanenko, V. N.; Verevkin, S. P.; Krol, O. V.; Varushchenko, R. M.; Chelovskaya, N. V. Vapour Pressures and Enthalpies of Vaporization of a Series of the Ferrocene Derivatives. *J. Chem. Thermodyn.* **2007**, *39*, 594–601.

(20) Monte, M. J. S.; Santos, L. M. N. B. F.; Fulem, M.; Fonseca, J. M. S.; Sousa, C. A. D. New Static Apparatus and Vapor Pressure of Reference Materials: Naphthalene, Benzoic Acid, Benzophenone, and Ferrocene. *J. Chem. Eng. Data* **2006**, *51*, 757–766.

(21) Pelino, M.; Tomassetti, M.; Piacente, V.; D'Ascenzo, G. Vapor Pressure Measurements of Ferrocene, mono- and 1,1′-di-Acetyl Ferrocene. *Thermochim. Acta* **1981**, *44*, 89–99.

(22) Köster, A. M.; Calaminici, P.; Casida, M. E.; Flores-Moreno, R.; Geudtner, G.; Goursot, A.; Heine, T.; Ipatov, A.; Janetzco, F.; del Campo, J. M.; Patchkovskii, S.; Reveles, J. U.; Vela, A. M.; Salahub, D. R. *deMon2k, The International deMon Developers Community*; University of Montreal: Montreal, Canada, 2007.

(23) Kohn, W.; Sham, L. Self-Consistent Equations Including Exchange and Correlation Effects. *Phys. Rev. A* **1965**, *140*, 1133–1138.

(24) Perdew, J. P.; Chevary, J. A.; Vosko, S. H.; Jackson, K. A.; Pederson, M. R.; Singh, D. J.; Fiolhais, C. Atoms, Molecules, Solids, and Surfaces: Applications of the Generalized Gradient Approximation for Exchange and Correlation. *Phys. Rev. B* **1992**, *46*, 6671–6687.

(25) Goudbout, N.; Salahub, D. R.; Andzelm, J.; Wimmer, E. Optimization of Gaussian-Type Basis Sets for Local Spin Density Functional Calculations. Part I. Boron through Neon, Optimization Technique and Validation. *Can. J. Phys.* **1992**, *70*, 560–571.

(26) Jug, K.; Janetzko, F.; Köster, A. M. Calculation of Heat Capacities and Entropies of Metal Halides with Quantum Chemical Methods. *J. Chem. Phys.* **2001**, *114*, 5472–5481.

(27) Bevington, P. R. *Data Reduction and Error Analysis for the Physical Sciences*; McGraw-Hill Book Company: New York, 1969.

(28) Turnbull, A. G. Thermochemistry of Biscyclopentsdienyl Metal Compounds. *Austral. J. Chem.* **1967**, *20*, 2757–2760.

(29) Chickos, J. S.; Hosseini, S.; Hesse, D. G.; Liebman, J. F. Heat Capacity Correction to a Standard State: A Comparison of New and Some Literature Methods for Organic Liquids and Solids. *Struct. Chem.* **1993**, *4*, 271–278.

(30) Rabinovich, I. B.; Nistratov, V. P.; Sheiman, M. S.; Burchalova, G. V. Heat Capacities of Dicyclopentadienyl Compounds of Vanadium, Chromium, Manganese, Cobalt, and Nickel. *J. Chem. Thermodyn.* **1978**, *10*, 523–536.

(31) Seiler, P.; Dunitz, J. D. The Structure of Nickelocene at Room Temperature and at 101 K. *Acta Crystallogr., Sect. B* **1980**, *36*, 2255–2260.

(32) Antipin, M. Y.; Boese, R.; Augart, N.; Schmid, G. Redetermination of the Cobaltocene Crystal Structure at 100 and 297 K: Comparison with Ferrocene and Nickelocene. *Struct. Chem.* **1993**, *4*, 91–101.

(33) Clec'h, G.; Calvarin, G. Etude Structurale des Phases Desordonnees de $Co(C_5H_5)_2$, $Mg(C_5H_5)_2$, et Transitions de Phases de $(C_4H_4)N$) Fe (C_5H_5). *Mol. Cryst. Liq. Cryst.* **1985**, *128*, 305–320.